Myeloid differentiation architecture of leukocyte transcriptome dynamics in perceived social isolation

Steven W. Cole[a,b], John P. Capitanio[c,d], Katie Chun[c,d], Jesusa M. G. Arevalo[a,b], Jeffrey Ma[a,b], and John T. Cacioppo[e,f,g,1]

[a]Division of Hematology-Oncology, Department of Medicine, University of California, Los Angeles School of Medicine, Los Angeles, CA 90095; [b]Norman Cousins Center, University of California, Los Angeles School of Medicine, Los Angeles, CA 90095; [c]Department of Psychology, University of California, Davis, CA 95616; [d]California National Primate Research Center, University of California, Davis, CA 95616; [e]Center for Cognitive and Social Neuroscience, University of Chicago, Chicago, IL 60637; [f]Department of Psychology, University of Chicago, Chicago, IL 60637; and [g]Department of Psychiatry and Behavioral Neuroscience, University of Chicago, Chicago, IL 60637

Edited by Burton H. Singer, University of Florida, Gainesville, FL, and approved October 21, 2015 (received for review July 21, 2015)

To define the cellular mechanisms of up-regulated inflammatory gene expression and down-regulated antiviral response in people experiencing perceived social isolation (loneliness), we conducted integrative analyses of leukocyte gene regulation in humans and rhesus macaques. Five longitudinal leukocyte transcriptome surveys in 141 older adults showed up-regulation of the sympathetic nervous system (SNS), monocyte population expansion, and up-regulation of the leukocyte conserved transcriptional response to adversity (CTRA). Mechanistic analyses in a macaque model of perceived social isolation confirmed CTRA activation and identified selective up-regulation of the CD14^{++}/CD16^{-} classical monocyte transcriptome, functional glucocorticoid desensitization, down-regulation of Type I and II interferons, and impaired response to infection by simian immunodeficiency virus (SIV). These analyses identify neuroendocrine-related alterations in myeloid cell population dynamics as a key mediator of CTRA transcriptome skewing, which may both propagate perceived social isolation and contribute to its associated health risks.

social genomics | loneliness | inflammation | health

Perceived social isolation (PSI) (loneliness in humans) is a risk factor for chronic illness and all-cause mortality (1, 2), but the molecular mechanisms of its health effects remain poorly understood. PSI represents a discrepancy between an animal's preferred and actual social relations and triggers phylogenetically conserved neuroendocrine responses (3–5). In humans, PSI involves an implicit hypervigilance for social threat (4–6). In animal models, threat-related signaling from the sympathetic nervous system (SNS) to the bone marrow hematopoietic niche can stimulate the development of immature, glucocorticoid-resistant monocytes and neutrophils (myeloid lineage immune cells) via β-adrenergic up-regulation of the myelopoietic growth factor, granulocyte-macrophage colony-stimulating factor (GM-CSF) (7, 8). Up-regulated myeloid cell populations may subsequently contribute to the development of inflammation-related chronic diseases (9). Here, we show that individuals chronically high in PSI manifest an SNS-related alteration in myeloid cell population dynamics that mediates a previously observed conserved transcriptional response to adversity (CTRA) involving up-regulation of proinflammatory genes and down-regulation of genes involved in type I interferon (IFN) responses. CTRA gene expression also predicts subsequent PSI, suggesting a reciprocal interaction between inflammatory biology and social perception. Mechanistic analyses in a macaque model of PSI (10) confirm CTRA activation, identify the CD14^{++}/CD16^{-} classical monocyte subpopulation as the cellular origin of that transcriptome shift, and document functional immunologic consequences, including reduced cellular sensitivity to glucocorticoid regulation, down-regulation of type I and II IFNs, and impaired response to infection with the simian immunodeficiency virus (SIV).

Results

To assess the role of myeloid lineage gene expression in PSI-related CTRA up-regulation (11–13), we analyzed 412 genome-wide transcriptome surveys of peripheral blood mononuclear cells (PBMCs) collected longitudinally from 141 participants in the Chicago Health, Aging, and Social Relations Study (CHASRS) (14) during study years 5, 7, 8, 9, and 10 (Table S1). This subsample was representative of the overall CHASRS cohort (14), and 26% were classified as chronically high in PSI based on a previously established criterion of UCLA Loneliness Scale scores ≥41 in at least 60% of study years 1–5 (12). (Trait PSI was defined before gene expression profiling to rule out reverse causation.) Participants chronically high in PSI did not differ from those intermediate or low in PSI on any measured demographic or health behavior risk factor (all Ps > 0.05). However, they did show greater levels of perceived stress and depressive symptoms and lower levels of social support (Table S1), as previously observed (15–17). In mixed effect linear model analyses relating chronically high PSI to a CTRA indicator gene contrast reflecting up-regulated inflammation and down-regulated type I IFN activity and antibody synthesis, results showed an average 6.5% elevation in the CTRA gene expression profile [adjusting for covariates: study year, age, sex, race/ethnicity, body mass index (BMI), smoking, alcohol consumption, and household income] (Table 1, row A and Fig. 1*A*). The CTRA profile was up-regulated by 12.2% after additional adjustments for stress, depression, and social support (Table 1, row B) whereas none of the latter three psychological risk factors was associated with increased CTRA expression (Table 1, row B).

Significance

Perceived social isolation (PSI) (loneliness) is linked to increased risk of chronic disease and mortality, and previous research has implicated up-regulated inflammation and down-regulated antiviral gene expression (the conserved transcriptional response to adversity; CTRA) as a potential mechanism for such effects. The present studies used integrative analyses of transcriptome regulation in high-PSI humans and rhesus macaques to define the basis for such effects in neuroendocrine-related alterations in myeloid immune cell population dynamics. CTRA up-regulation also preceded increases in PSI, suggesting a reciprocal mechanism by which CTRA gene expression may both propagate PSI and contribute to its related disease risks.

Author contributions: S.W.C., J.P.C., and J.T.C. designed research; S.W.C., J.P.C., K.C., J.M.G.A., J.M., and J.T.C. performed research; S.W.C. contributed new reagents/analytic tools; S.W.C., J.P.C., and J.T.C. analyzed data; and S.W.C., J.P.C., and J.T.C. wrote the paper.

The authors declare no conflict of interest.

This article is a PNAS Direct Submission.

Freely available online through the PNAS open access option.

Data deposition: The data reported in this paper have been deposited in the Gene Expression Omnibus (GEO) database, www.ncbi.nlm.nih.gov/geo (accession nos. GSE65213, GSE65298, GSE65317, GSE65341, GSE65403, and GSE65243).

[1]To whom correspondence should be addressed. Email: Cacioppo@uchicago.edu.

This article contains supporting information online at www.pnas.org/lookup/suppl/doi:10.1073/pnas.1514249112/-/DCSupplemental.

Table 1. Perceived social isolation (PSI), monocyte percentages, and CTRA gene expression

Outcome	Association $b \pm$ SE*	Test statistic	*P* value
A. CTRA gene expression[†]			
Chronic PSI[‡]	0.091 ± 0.040	$F(1,2E4) = 5.22$	0.0239
B. CTRA gene expression[†]			
Chronic PSI[‡]	0.166 ± 0.044	$F(1,2E4) = 14.44$	0.0002
Depressive symptoms (CESD)	−0.003 ± 0.002	$F(1,2E4) = 2.01$	0.1559
Stress (PSS)	−0.005 ± 0.002	$F(1,2E4) = 6.57$	0.0104
Social support (ISEL)	0.011 ± 0.007	$F(1,2E4) = 2.51$	0.1134
C. CTRA gene expression[†]			
Concurrent continuous PSI[§]	0.013 ± 0.002	$F(1,1E4) = 28.81$	0.0001
1-y antecedent continuous PSI[§]	0.007 ± 0.002	$F(1,1E4) = 11.24$	0.0008
D. CTRA gene expression[†]			
Chronic PSI[‡]	−0.232 ± 0.127	$F(1,1E4) = 3.33$	0.0705
Concurrent continuous PSI[§]	0.014 ± 0.002	$F(1,1E4) = 31.43$	< 0.0001
1-y antecedent continuous PSI[§]	0.008 ± 0.002	$F(1,1E4) = 13.19$	0.0003
E. PSI[§]			
Concurrent CTRA gene expression[†]	0.137 ± 0.036	$F(1,9E3) = 14.53$	0.0001
1-y antecedent CTRA gene expression[†]	0.202 ± 0.034	$F(1,9E3) = 35.16$	< 0.0001
F. Monocyte %[¶]			
Chronic PSI[‡]	0.833 ± 0.423	$F(1,76) = 3.87$	0.0520
Concurrent continuous PSI[§]	0.057 ± 0.022	$F(1,76) = 6.58$	0.0123
G. CTRA gene expression[†]			
Monocyte %[¶]	0.021 ± 0.006	$F(1,9E3) = 11.57$	0.0007
H. CTRA gene expression[†]			
Leukocyte subset marker mRNA[#]	n/a	$F(8,2E4) = 7.88$	< 0.0001
I. CTRA gene expression[†]			
Chronic PSI|leukocyte subset mRNA[#]	0.102 ± 0.041	$F(1,2E4) = 6.19$	0.0141
Leukocyte subset mRNA[#]|chronic PSI[¶]	n/a	$F(8,2E4) = 8.00$	< 0.0001

CESD, Center for Epidemiological Studies Depression; ISEL, Interpersonal Support Evaluation List; PSS, Perceived Stress Scale.

*Partial regression coefficients relating listed predictor variables to listed outcomes, with additional control for age, sex, race (white, black, Hispanic), marital status, (log) household income, BMI, smoking, and alcohol consumption. n/a, not applicable.

[†]Standardized expression values (mean = 0, SD = 1) for 53 CTRA indicator genes.

[‡]1/0 indicator.

[§]Continuous UCLA Loneliness Scale scores: mean = 36.5, SD = 8.9. Association parameter represents change in expected UCLA Loneliness Scale score per log2 unit change in average CTRA gene expression level.

[¶]Monocyte %: mean = 8.5, SD = 2.1.

[#]Standardized expression values (mean = 0, SD = 1) for mRNAs encoding *CD14*, *CD3D*, *CD3E*, *CD4*, *CD8*, *CD19*, CD16/*FCGR3A*, and CD56/*NCAM1*.

To determine whether high PSI might constitute an antecedent influence on CTRA expression, analyses examined relationships between longitudinal variations in continuous Loneliness Scale scores measured concurrently and 1 y before observed gene expression values in the entire study cohort (again controlling for covariates and stress, depression, and social support). CTRA gene expression was up-regulated in proportion to both concurrent and 1-y-antecedent PSI (Table 1, row C), and these effects emerged above and beyond individual differences in chronic (trait) high PSI (Table 1, row D).

Inflammation may potentially influence PSI (18–20) so we also examined the reciprocal effects of concurrent and 1-y-antecedent CTRA expression on continuous PSI measures (Table 1, row E). PSI was elevated in proportion to both concurrent and 1-y-antecedent CTRA expression, suggesting a reciprocal relationship between social cognition and immune system gene regulation (19).

Monocyte Population Dynamics. Chronic social threat perception may up-regulate CTRA gene expression via SNS stimulation of bone marrow myelopoiesis and consequent up-regulation of immature, proinflammatory classical monocytes ($CD14^{++}/CD16^{-}$) in circulating PBMCs (7, 8). Both categorical chronic PSI and longitudinal variations in state PSI were associated with increased circulating monocyte percentages (again controlling for covariates; cell percentage is the hematologic parameter relevant to dynamics of a fixed-mass RNA transcriptome) (Fig. 1*B* and Table 1, row F). In turn, increased circulating monocyte percentages were associated with CTRA up-regulation (Fig. 1*C* and Table 1, row G), as were canonical mRNA markers of major leukocyte subsets including the monocyte marker *CD14* (Table 1, row H). However, control for leukocyte subset indicators could not account for the entire relationship between chronically high PSI and CTRA up-regulation (Table 1, row I). These results suggest that CTRA up-regulation may be mediated not by expansion of the total $CD14^{+}$ monocyte population, but rather by selective expansion of the immature $CD14^{++}/CD16^{-}$ classical monocyte subset (7, 8).

Consistent with neuronal SNS regulation of myelopoiesis (7, 8), longitudinal variations in state PSI were associated with concurrent elevations in urinary norepinephrine metabolites (indicative of neuronal SNS activity) (Fig. 1*D*) but not with epinephrine (indicative of adrenal SNS activity) (Fig. 1*D*). Cortisol levels were also up-regulated in chronic high PSI (Fig. 1*D*), as previously observed (4).

Macaque Model. To facilitate mechanistic analyses of PSI-related immunologic and behavioral processes, we established a rhesus macaque model that distinguished behaviorally between animals high in PSI versus controls (i.e., animals low or intermediate in PSI) based on (*i*) high vs. low rates of spontaneous social interaction and (*ii*) subdivision of low-social interaction animals into social threat-sensitive and -insensitive groups based on patterns of threat discrimination in spontaneous social behavior (i.e., a bias to

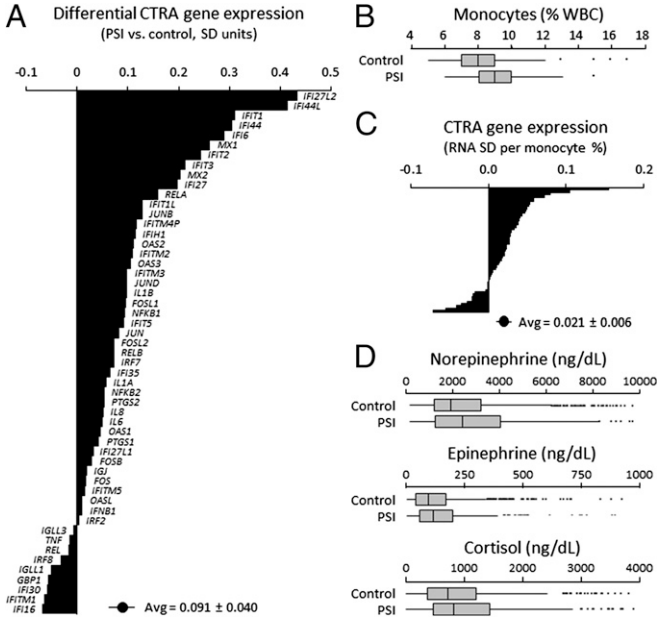

Fig. 1. CTRA gene expression, monocyte prevalence, and neuroendocrine parameters in individuals chronically high in PSI. (*A*) Differential expression of 53 CTRA indicator transcripts in five yearly longitudinal PBMC samples from individuals chronically high in PSI ($n = 36$) vs. those intermediate or low in PSI ($n = 105$). Point estimates and SE come from repeated measures mixed effect linear models ($P = 0.024$, as in Table 1, row A). (*B*) Monocyte percentages in two longitudinal whole blood samples from individuals chronically high versus intermediate or low in PSI (association with categorical chronically high PSI, $P = 0.052$; association with continuously varying PSI as measured by UCLA Loneliness Scale scores, $P = 0.012$). Boxes, 25th, 50th, and 75th percentiles; whiskers, first and 99th percentiles. (*C*) CTRA gene expression as a function of monocyte percentage (association, $P < 0.001$ by repeated measures mixed linear model). (*D*) PSI-related differences in urinary metabolite concentrations for norepinephrine (association with categorical chronic high PSI, $b = 332.1 \pm$ SE 194.7 ng/dL, $P = 0.090$; association with continuous PSI, $b = 23.0 \pm 7.4$ ng/dL, $P = 0.002$), epinephrine (categorical, $b = 16.0 \pm 12.2$ ng/dL, $P = 0.192$; continuous, $b = 0.4 \pm 0.5$ ng/dL, $P = 0.401$), and cortisol (categorical, $b = 197.5 \pm 83.6$ ng/dL, $P = 0.018$; continuous, $b = 5.4 \pm 3.6$ ng/dL, $P = 0.134$).

approach safe social targets such as juveniles or adult females vs. risky adult males, and inability to convert social initiations into complex social interactions such as grooming), as described (10). The resulting classification yields categories of low PSI (high sociability), intermediate PSI (low sociability, low social threat sensitivity), and high PSI (low sociability, high social threat sensitivity). Macaque PSI classification was relatively stable over time (1 y test–retest, $\kappa = 0.51$ in 30 animals) and similar to PSI stability in humans (mean 1 y test–retest reliability of UCLA Loneliness score of ≥ 41, $\kappa = 0.56$). Behavioral homology of the macaque model to human PSI was verified by assessing individual differences in behavioral sensitivity to social threat in 27 animals (high PSI, $n = 7$; intermediate PSI, $n = 10$; low PSI, $n = 10$). High-PSI macaques produced higher rates of preference-indicating behavior in response to video-presented affiliative behaviors generated by novel safe (juvenile) vs. risky (adult) male social partners whereas low-PSI animals showed no such target-based response discrimination (Fig. 2*A*). Social threat-sensitive behavioral response biases habituated over three daily exposure sessions, confirming that response biases stemmed from social novelty rather than an inherent preference for juveniles per se (Fig. 2*A*). In analyses of archival data on urinary catecholamine metabolites from a previous study of 18 adult male macaques (21), high-PSI macaques were also homologous to human PSI in showing elevated norepinephrine but no differences in epinephrine (Fig. 2*B*).

In analyses of genome-wide transcriptional profiles from a new sample of 49 macaques (high PSI, $n = 8$; intermediate PSI, $n = 19$; low PSI, $n = 22$), mixed effect linear model analyses found high-PSI macaques to parallel high-PSI humans in showing up-regulated CTRA expression within the PBMC pool (Fig. 3*A*) (contrast with low- and intermediate-PSI animals, $b = 0.206 \pm 0.081$ standardized RNA expression units, $P = 0.0147$). Transcript origin analyses (TOA) (12) of all genes showing $\geq$1.2-fold differential expression in high- vs. low- and intermediate-PSI animals confirmed that PBMC transcriptome differences originated predominantly from monocytes (Fig. 3*B*). Additional TOAs using isolated $CD14^{++}/CD16^{-}$ and $CD14^{+}/CD16^{+}$ monocyte samples as dimensional reference points confirmed that PBMC transcriptome differences originated specifically from the $CD14^{++}/CD16^{-}$ classical monocyte subset (Fig. 3*C*).

Consistent with previous analyses of high-PSI humans (11, 22) and socially stressed mice (7, 23–26), circulating immune cells from high-PSI macaques also showed reduced glucocorticoid receptor (GR) functional activity, including blunted neutrophil redistribution response to endogenous diurnal variation in cortisol levels (Fig. 3*D*) and bioinformatic indications of down-regulated GR transcriptional activity and reciprocal up-regulation of NF-κB (which is generally inhibited by GR signaling) (Fig. 3*E*).

To determine whether chronically experienced social threat (a central mechanism of human chronic PSI) (4–6) can causally impact monocyte population dynamics, we analyzed archival hematologic data from a previous study in which 21 individually housed adult male macaques were randomized to socialize for 100 min/d on 3–5 d/wk with either a continually varying array of novel social partners or a stable group of social partners (21). Relative to the familiar contact control condition, animals exposed to chronic social novelty over 5 wk showed up-regulated prevalence of circulating monocytes in general (Fig. 4*A*) and $CD14^{++}/CD16^{-}$ classical monocytes in particular (Fig. 4*B*). $CD14^{+}/CD16^{++}$ nonclassical monocytes were not significantly expanded (Fig. 4*B*).

To assess the functional significance of PSI-related alterations in myeloid transcriptome regulation, we surveyed expression of type I and II IFNs in an additional sample of 17 macaques under basal physiologic conditions and after experimental infection with SIV. At baseline (2 wk preinfection), high-PSI animals showed up-regulated circulating monocyte frequencies (high PSI, mean $\pm$ SE, 544 $\pm$ 103 cells per mm^3; low and intermediate PSI

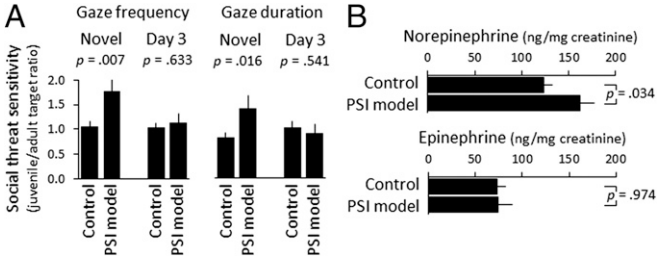

Fig. 2. Perceived social isolation, social threat, and SNS activity. (*A*) Behavioral indicators of preference (gaze frequency and duration) were assessed in 27 adult macaques classified as high PSI ($n = 7$), intermediate PSI ($n = 10$), and low PSI ($n = 10$) as they viewed video presentations of affiliative behavior directed at them by a novel safe juvenile male or risky adult male. Data represent mean $\pm$ SE threat discrimination ratios (juvenile target/adult target) on the first day of video exposure (novel social situation) and the third day (habituated) in high-PSI animals vs. intermediate- and low-PSI controls; *P* values from mixed effects linear model analysis of log-ratios. (*B*) Average urinary catecholamine metabolite concentrations in 18 adult male macaques classified as high PSI ($n = 4$) vs. intermediate- ($n = 6$) or low-PSI ($n = 8$) controls. Data come from archival analysis of newly derived PSI classifications in a previously published study (21) and represent mean $\pm$ SE of up to six assessments over 20 wk; *P* values indicate group main effect for each metabolite.

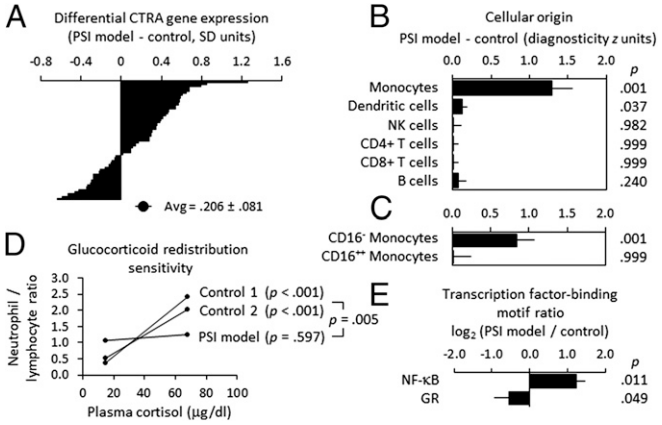

Fig. 3. Differential gene expression, monocyte transcriptome representation, and glucocorticoid regulation in the rhesus macaque model of PSI. (*A*) Differential expression of 53 CTRA indicator transcripts in PBMC samples from 49 rhesus macaques classified by behavioral observations as low or intermediate PSI (n = 22 and 19, respectively) vs. high PSI (n = 8) as in Fig. 1*A* (P = 0.017, controlling for age). (*B*) Transcript origin analyses (12) identifying major leukocyte subset origins of the 229 gene transcripts that showed ≥1.2-fold differential expression in high-PSI vs. intermediate- and low-PSI animals (70 up-regulated transcripts and 159 down-regulated transcripts are listed in Table S1). (*C*) Transcript origin analyses assessing the extent to which $CD14^{++}/CD16^{-}$ classical and $CD14^{+}/CD16^{+}$ nonclassical monocyte transcriptomes contributed to differential gene expression. (*D*) Functional glucocorticoid sensitivity of myeloid lineage immune cells (neutrophils) was assessed using an in vivo hematological redistribution assay that quantified the extent to which circulating neutrophil numbers (normalized to lymphocyte numbers to control for variations in total white blood cell count) varied as a function of endogenous physiological variations in cortisol levels (22, 24). Log-transformed neutrophil/lymphocyte ratios were subject to mixed effect linear model analysis of four repeated measurements collected at 9:00 AM and 3:00 PM on 2 d from low-PSI animals (n = 172 observations on 27 animals, 16 of whom were also resampled 1 y later), intermediate-PSI animals (n = 132 observations on 21 animals, 12 of whom were resampled 1 y later), and high-PSI animals (n = 32 observations on 6 animals, 2 of whom were resampled 1 y later). Average values are displayed in raw ratio units to facilitate interpretation, and lines span the observed range of cortisol values. (*E*) In vivo transcriptional activity of glucocorticoid receptor (GR) and NF-κB transcription factors as assessed by TELiS bioinformatic analysis (50) of transcription factor-binding motif prevalence in promoter DNA sequences of genes showing ≥1.2-fold differential gene expression in high-PSI animals vs. low- and intermediate-PSI controls.

controls, 295 ± 46; P = 0.0465) and percentages (high PSI, 4.5 ± 0.9%; controls, 2.5 ± 0.4%; P = 0.0540). Within the monocyte population, high-PSI animals also showed up-regulation of $CD14^{++}/CD16^{-}$ classical monocytes (413 ± 71 cells per mm^3 blood vs. 230 ± 29 in controls; P = 0.0310) but no difference in $CD14^{+}/CD16^{++}$ nonclassical monocytes (71 ± 71 cells per mm^3 vs. 22 ± 29; P = 0.5393). At baseline, high-PSI animals showed PBMC mRNA levels of *IFNA*, *IFNB*, and *IFNG* that were down-regulated by an average of 82%, 48%, and 92%, respectively, compared with controls (Fig. 5*A*). At 2 wk postinfection (peak of acute viral replication), IFN gene expression was significantly up-regulated across all groups (average > fourfold across all 3 *IFN*s; P < 0.0001) and did not differ significantly in high-PSI animals (Fig. 5*A*). At 10 wk postinfection, after the establishment of a long-term viral replication set point, high-PSI animals again showed reduced *IFN* gene expression (*IFNA* down-regulated by 64%, *IFNB* by 86%, and *IFNG* by 77%) (Fig. 5*A*). Presumably as a consequence of this impaired antiviral response, high-PSI animals also showed poorer suppression of PBMC SIV gene expression from the 2-wk peak of acute viral replication to the long-term viral replication set point at 10 wk postinfection (Fig. 5*B*), as well as elevated SIV viral load set point in plasma and cerebrospinal fluid (Fig. 5*C*) and reduced anti-SIV IgG antibody titers (Fig. 5*D*).

Discussion

These results show that the CTRA gene expression profile observed in PBMCs from chronically lonely individuals (11–13) is mediated by selective up-regulation of the $CD14^{++}/CD16^{-}$ classical monocyte transcriptome. Lonely people showed elevated SNS and hypothalamus-pituitary-adrenal–axis activity, relative expansion of the circulating monocyte pool, and monocyte-related activation of the CTRA transcriptome profile marked by up-regulated expression of proinflammatory genes and down-regulated expression of type I IFN- and antibody-related genes (4, 7, 19, 27). However, CTRA transcriptome skewing was not mediated by expansion of the total monocyte pool. Instead, analyses of gene regulation and cellular function in the macaque model of PSI (10) identified selective expansion of the $CD14^{++}/CD16^{-}$ classical monocyte subset as the primary mechanism of CTRA up-regulation. High-PSI macaques also showed heightened sensitivity to social threat, elevated SNS activity, down-regulated type I and II IFNs under basal conditions, impaired response to infectious challenge with SIV, and reduced cellular sensitivity to regulation by endogenous glucocorticoids (i.e., blunted redistribution responses to endogenous cortisol variations; reduced GR target gene expression; and reciprocal up-regulation of NF-κB target genes, which are normally inhibited by GR activation). Experimental studies in macaques also confirmed that $CD14^{++}/CD16^{-}$ classical monocytes can be causally up-regulated by chronic exposure to novelty-related social threat, which constitutes a central psychological mechanism of human chronic PSI (4–6). Collectively, these results support a mechanistic model in which lonely individuals' chronic perception of social threat (6) results in SNS-mediated up-regulation of myelopoiesis (7, 8) and a consequent increase in the prevalence of immature, inflammation-primed, IFN-impaired, and glucocorticoid-insensitive myeloid-lineage immune cells within the circulating leukocyte pool. The associated cell-intrinsic glucocorticoid insensitivity may explain how lonely individuals can show up-regulated proinflammatory gene expression despite concurrent elevations in systemic cortisol levels (which generally exert anti-inflammatory effects) (28–32); reduced GR signaling activity may leave the myeloid lineage immune cells of lonely individuals relatively insensitive to the antiinflammatory effects of endogenous glucocorticoids.

The present longitudinal associations also suggest that CTRA gene expression may reciprocally influence PSI. Up-regulation of circulating immature monocytes provides a plausible mechanism for such effects through the known ability of these cells to traffic into the brain where they act to promote anxiety and alter social behavior (33). Proinflammatory cytokines can also circulate to the brain to activate "sickness behaviors" (19, 34) that include affective, motivational, and perceptual processes that may amplify PSI and reduce social engagement (18–20). Inflammation-mediated reciprocal regulation could act to amplify or prolong

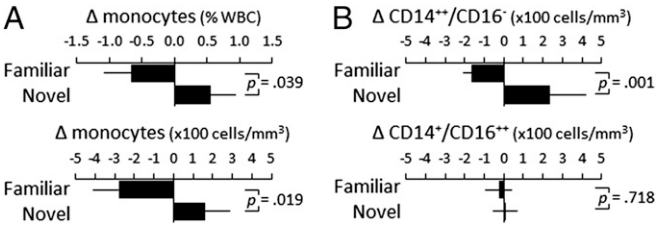

Fig. 4. Social threat and monocyte population dynamics. Effect of chronic novelty-related social threat on circulating monocyte populations was assessed in 21 adult male macaques randomized to socialize for 100 min/d on 3–5 d/wk with either a continually varying array of novel social partners (n = 11) or a stable group of social partners (n = 10) (21). Data represent mean ± SE change from presocialization baseline to 5-wk follow-up in total monocytes (*A*) and classical and nonclassical monocyte subsets (*B*); P values from mixed effect linear model analysis.

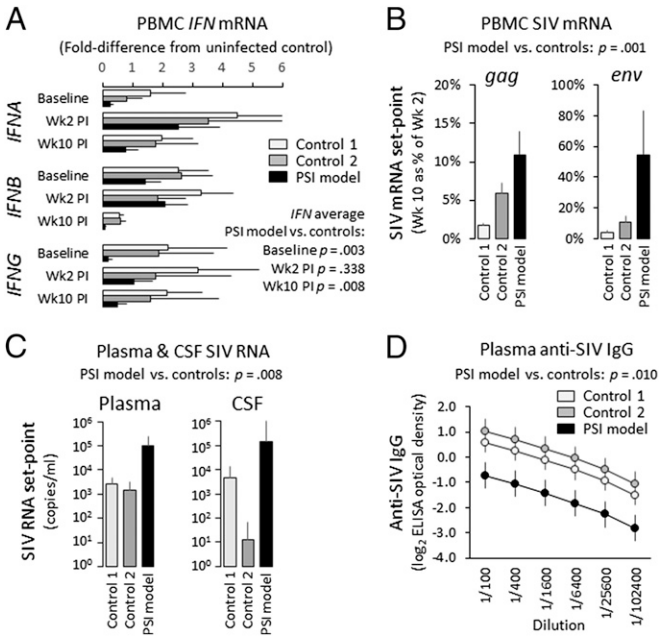

Fig. 5. IFN gene expression and response to SIV infection in the rhesus macaque model of PSI. (*A*) mRNA encoding type I (*IFNA*, *IFNB*) and type II (*IFNG*) interferons was assessed in PBMCs from 12 adult male macaques experimentally infected with simian immunodeficiency virus (SIV) (Control 1, 6 low PSI; Control 2, 4 intermediate PSI; PSI model: 2 high PSI) at preinfection baseline, 2 wk postinfection (peak of acute viral replication), and 10 wk postinfection (long-term viral replication set point). Data represent mean ± SE fold-difference from five SIV-uninfected controls; *P* values contrast high-PSI vs. controls pooling across *IFN*s. (*B*) Immunologic response to SIV was assessed by quantifying suppression of SIV *gag* and *env* mRNA levels in PBMC from peak viral replication (wk 2 postinfection) to long-term set point (wk 10). Data represent mean ± SE % reduction from wk 2 to wk 10; *P* value contrasts high-PSI vs. controls pooling across SIV transcripts. Long-term control of viral replication was assessed by plasma SIV viral load (*C*) and anti-SIV IgG titers (*D*) at set point (wk 10). Data represent mean ± SE $\log_{10}$ SIV RNA copies per milliliter of plasma or $\log_2$ optical density of IgG ELISA over fourfold plasma dilutions; *P* values contrast high-PSI vs. controls.

socially originated PSI (35). However, the fact that these reciprocal associations emerge above and beyond the general effects of chronic (trait) PSI also implies that behavioral interventions to reduce PSI may trigger concomitant biological changes that help propagate social integration (as well as reduced CTRA gene expression) (13).

These findings are limited by the correlational design of the human longitudinal study and the macaque PSI model (PSI may constitute both a cause and an effect of CTRA gene expression, and both may be commonly regulated by neural, endocrine, or epigenetic dynamics). This study was not designed to discover individual genes associated with PSI, and PSI may relate to other transcriptome dynamics that remain to be identified in future studies (e.g., blood informative transcript axes) (36). These results are consistent with epidemiologic data linking PSI to disease risk (1, 2, 37, 38). However, experimental manipulations of PSI, SNS activity, and myelopoiesis will be required to more fully define the molecular mechanisms and health significance of these effects. In addition to myelopoiesis (7, 8), the SNS may also regulate CTRA expression via per-cell transcriptional alterations (e.g., β-adrenergic inhibition of *IFN* gene transcription) (39, 40) or transient mobilization of nonclassical monocytes from the vascular margin (41). However, the latter dynamic cannot account for the present effects because acute SNS activation mobilizes nonclassical monocytes (41) whereas classical monocytes were up-regulated here. It is also important to note that the present analysis does not hypothesize any change in gene expression within classical vs. nonclassical monocytes (i.e., on a per-cell basis), only an increase in the relative prevalence of the (per-cell fixed) classical monocyte transcriptome within the overall PBMC pool. Future research will be required to confirm the specific neuroimmune interactions mediating these monocyte population dynamics. This study's molecular, cellular, behavioral, and immunologic validation of a macaque model of human PSI provides a useful experimental system for mapping the causal interactions among social perception, neural activity, immunologic function, and health.

Methods

Human Neuroendocrine, Immune, and Transcriptome Parameters. Data came from the Chicago Health, Aging, and Social Relations Study (CHASRS) (14, 42). Overnight urine concentrations of cortisol, epinephrine, and norepinephrine were determined by HPLC (14), monocyte prevalence by automated complete blood counts (CBCs), and peripheral blood mononuclear cell (PBMC) transcriptome profiles by Illumina bead array assays for all 144 participants who provided a blood sample for RNA assessment during CHASRS years 5, 7, 8, 9, or 10 (12). Year 5, 7, and 8 samples were assayed by Ref8 arrays (Gene Expression Omnibus Series GSE65213, GSE65298, and GSE65317), year 9–10 samples were assayed by HT-12 BeadArrays (GSE65341 and GSE65403), and CTRA gene expression was analyzed using mixed effect linear models (43) testing association between average expression of 53 CTRA indicator transcripts (44, 45) and either continuous UCLA Loneliness Scale scores or a 1/0 indicator of chronically high PSI (12) (UCLA Loneliness Scale score of ≥41 in at least 60% of measurements taken during study years 1–5) while controlling for study year, age, sex, race/ethnicity, marital status, household income, BMI, alcohol consumption, smoking history, and gene-specific differences in average expression level. Written informed consent was obtained from all study participants after the nature of this research was explained and all participant questions were addressed, and all procedures were approved by the Institutional Review Board of the University of Chicago. Additional analytic details are available in *SI Methods*.

Macaque Neuroendocrine, Hematologic, and Transcriptome Parameters. Animals were classified as high, intermediate, or low PSI based on (*i*) high (>0.5 SD above mean) and low (>0.5 SD below mean) levels of ethologically assessed sociability and (*ii*) subdivision of low-sociable animals based on social threat discrimination in approach behavior (i.e., preferential approach to safe juveniles or females vs. risky adult males), yielding low PSI (high sociability), intermediate PSI (low sociability, low social threat sensitivity), and high PSI classifications (low sociability, high social threat sensitivity) (10). Homology to social threat perception in human chronic PSI (4–6, 10) was assessed by behavioral response to videos depicting a novel safe (juvenile) vs. threatening (adult) male macaque. Urinary catecholamine metabolite levels and hematologic responses to experimentally imposed chronic social novelty were assessed in archival data from two published studies (21) by applying PSI classification to archival social behavior data. For transcriptome analyses, PBMCs from a new sample of 56 PSI-classified macaques were assayed by Illumina bead arrays (46)(GSE65243); the 53-gene CTRA indicator profile was analyzed by mixed effect linear models controlling for age; and bioinformatic analyses of all transcripts showing ≥1.2-fold differential expression between high-PSI and the average of low- and medium-PSI assessed (*i*) the cellular origins of differential gene expression using transcript origin analysis (12) [mapped to major leukocyte subsets (47, 48) or $CD14^{++}/CD16^{-}$ vs. $CD14^{+}/CD16^{++}$ monocytes (49)] and (*ii*) functional glucocorticoid insensitivity using Transcription Element Listening System (TELiS) analysis of GR and NF-κB response element distribution (50). Functional glucocorticoid sensitivity was verified by neutrophil redistribution sensitivity to diurnal cortisol variation (22, 24). Antiviral response was assessed by inoculating macaques with SIV_{mac251} (or saline control) and assessing PBMC mRNA for *IFNA*, *IFNB*, *IFNG*, and SIV *gag* and *env* at baseline and 2 wk and 10 wk postinfection (21, 51), plasma SIV viral load set point (52, 53), and IgG antibody titers (54). All procedures were approved by the Institutional Animal Care and Use Committee of the California National Primate Research Center. *SI Methods* contains additional details.

ACKNOWLEDGMENTS. We thank Emma Adam, Louise Hawkley, HsiYuan Chen, Erna Tarara, and the University of California, Los Angeles Neuroscience Genomics Core for assistance. This study was supported by National Institutes of Health Grants R37-AG033590, P01-AG18911, R01-AG034052, R01-AG043404, P30-AG017265, P30-AG028748, R01-DA024441, and P51-OD011107; the Mind, Body, Brain and Health Initiative of the John D. and Catherine T. MacArthur Foundation; and the John Templeton Foundation.

1. Holt-Lunstad J, Smith TB, Layton JB (2010) Social relationships and mortality risk: A meta-analytic review. *PLoS Med* 7(7):e1000316.
2. Luo Y, Hawkley LC, Waite LJ, Cacioppo JT (2012) Loneliness, health, and mortality in old age: A national longitudinal study. *Soc Sci Med* 74(6):907–914.
3. Cacioppo S, Capitanio JP, Cacioppo JT (2014) Toward a neurology of loneliness. *Psychol Bull* 140(6):1464–1504.
4. Cacioppo JT, Cacioppo S, Capitanio JP, Cole SW (2015) The neuroendocrinology of social isolation. *Annu Rev Psychol* 66:733–767.
5. Cacioppo JT, et al. (2015) Loneliness across phylogeny and a call for comparative studies and animal models. *Perspect Psychol Sci* 10(2):202–212.
6. Cacioppo JT, Hawkley LC (2009) Perceived social isolation and cognition. *Trends Cogn Sci* 13(10):447–454.
7. Powell ND, et al. (2013) Social stress up-regulates inflammatory gene expression in the leukocyte transcriptome via β-adrenergic induction of myelopoiesis. *Proc Natl Acad Sci USA* 110(41):16574–16579.
8. Heidt T, et al. (2014) Chronic variable stress activates hematopoietic stem cells. *Nat Med* 20(7):754–758.
9. Finch CE (2007) *The Biology of Human Longevity: Inflammation, Nutrition, and Aging in the Evolution of Lifespans* (Academic, Burlington, MA).
10. Capitanio JP, Hawkley LC, Cole SW, Cacioppo JT (2014) A behavioral taxonomy of loneliness in humans and rhesus monkeys (Macaca mulatta). *PLoS One* 9(10):e110307.
11. Cole SW, et al. (2007) Social regulation of gene expression in human leukocytes. *Genome Biol* 8(9):R189.
12. Cole SW, Hawkley LC, Arevalo JM, Cacioppo JT (2011) Transcript origin analysis identifies antigen-presenting cells as primary targets of socially regulated gene expression in leukocytes. *Proc Natl Acad Sci USA* 108(7):3080–3085.
13. Creswell JD, et al. (2012) Mindfulness-based stress reduction training reduces loneliness and pro-inflammatory gene expression in older adults: A small randomized controlled trial. *Brain Behav Immun* 26(7):1095–1101.
14. Hawkley LC, Masi CM, Berry JD, Cacioppo JT (2006) Loneliness is a unique predictor of age-related differences in systolic blood pressure. *Psychol Aging* 21(1):152–164.
15. Hawkley LC, Burleson MH, Berntson GG, Cacioppo JT (2003) Loneliness in everyday life: Cardiovascular activity, psychosocial context, and health behaviors. *J Pers Soc Psychol* 85(1):105–120.
16. Steptoe A, Owen N, Kunz-Ebrecht SR, Brydon L (2004) Loneliness and neuroendocrine, cardiovascular, and inflammatory stress responses in middle-aged men and women. *Psychoneuroendocrinology* 29(5):593–611.
17. Cacioppo JT, Hughes ME, Waite LJ, Hawkley LC, Thisted RA (2006) Loneliness as a specific risk factor for depressive symptoms: Cross-sectional and longitudinal analyses. *Psychol Aging* 21(1):140–151.
18. Eisenberger NI, Inagaki TK, Mashal NM, Irwin MR (2010) Inflammation and social experience: An inflammatory challenge induces feelings of social disconnection in addition to depressed mood. *Brain Behav Immun* 24(4):558–563.
19. Irwin MR, Cole SW (2011) Reciprocal regulation of the neural and innate immune systems. *Nat Rev Immunol* 11(9):625–632.
20. Inagaki TK, Muscatell KA, Irwin MR, Cole SW, Eisenberger NI (2012) Inflammation selectively enhances amygdala activity to socially threatening images. *Neuroimage* 59(4):3222–3226.
21. Capitanio JP, Cole SW (2015) Social instability and immunity in rhesus monkeys: the role of the sympathetic nervous system. *Philos Trans R Soc Lond B Biol Sci* 370(1669): 370.
22. Cole SW (2008) Social regulation of leukocyte homeostasis: The role of glucocorticoid sensitivity. *Brain Behav Immun* 22(7):1049–1055.
23. Stark JL, et al. (2001) Social stress induces glucocorticoid resistance in macrophages. *Am J Physiol Regul Integr Comp Physiol* 280(6):R1799–R1805.
24. Cole SW, Mendoza SP, Capitanio JP (2009) Social stress desensitizes lymphocytes to regulation by endogenous glucocorticoids: Insights from in vivo cell trafficking dynamics in rhesus macaques. *Psychosom Med* 71(6):591–597.
25. Wohleb ES, et al. (2011) β-Adrenergic receptor antagonism prevents anxiety-like behavior and microglial reactivity induced by repeated social defeat. *J Neurosci* 31(17):6277–6288.
26. Hanke ML, Powell ND, Stiner LM, Bailey MT, Sheridan JF (2012) Beta adrenergic blockade decreases the immunomodulatory effects of social disruption stress. *Brain Behav Immun* 26(7):1150–1159.
27. Cole SW (2014) Human social genomics. *PLoS Genet* 10(8):e1004601.
28. Miller GE, Cohen S, Ritchey AK (2002) Chronic psychological stress and the regulation of pro-inflammatory cytokines: A glucocorticoid-resistance model. *Health Psychol* 21(6):531–541.
29. Pace TW, Hu F, Miller AH (2007) Cytokine-effects on glucocorticoid receptor function: relevance to glucocorticoid resistance and the pathophysiology and treatment of major depression. *Brain Behav Immun* 21(1):9–19.
30. Miller GE, et al. (2008) A functional genomic fingerprint of chronic stress in humans: Blunted glucocorticoid and increased NF-kappaB signaling. *Biol Psychiatry* 64(4): 266–272.
31. Miller GE, et al. (2009) Low early-life social class leaves a biological residue manifested by decreased glucocorticoid and increased proinflammatory signaling. *Proc Natl Acad Sci USA* 106(34):14716–14721.
32. Miller GE, et al. (2014) Greater inflammatory activity and blunted glucocorticoid signaling in monocytes of chronically stressed caregivers. *Brain Behav Immun* 41: 191–199.
33. Wohleb ES, McKim DB, Sheridan JF, Godbout JP (2014) Monocyte trafficking to the brain with stress and inflammation: A novel axis of immune-to-brain communication that influences mood and behavior. *Front Neurosci* 8:447.
34. Dantzer R, O'Connor JC, Freund GG, Johnson RW, Kelley KW (2008) From inflammation to sickness and depression: When the immune system subjugates the brain. *Nat Rev Neurosci* 9(1):46–56.
35. Hawkley LC, et al. (2008) From social structure factors to perceptions of relationship quality and loneliness: The Chicago Health, Aging, and Social Relations Study. J Gerontol Soc Sci 63B(6):S375–S384.
36. Preininger M, et al. (2013) Blood-informative transcripts define nine common axes of peripheral blood gene expression. *PLoS Genet* 9(3):e1003362.
37. Holwerda TJ, et al. (2012) Increased risk of mortality associated with social isolation in older men: only when feeling lonely? Results from the Amsterdam Study of the Elderly (AMSTEL). *Psychol Med* 42(4):843–853.
38. Luo Y, Waite LJ (2014) Loneliness and mortality among older adults in China. *J Gerontol B Psychol Sci Soc Sci* 69(4):633–645.
39. Cole SW, Korin YD, Fahey JL, Zack JA (1998) Norepinephrine accelerates HIV replication via protein kinase A-dependent effects on cytokine production. *J Immunol* 161(2):610–616.
40. Collado-Hidalgo A, Sung C, Cole S (2006) Adrenergic inhibition of innate anti-viral response: PKA blockade of Type I interferon gene transcription mediates catecholamine support for HIV-1 replication. *Brain Behav Immun* 20(6):552–563.
41. Dimitrov S, et al. (2013) Differential TNF production by monocyte subsets under physical stress: Blunted mobilization of proinflammatory monocytes in prehypertensive individuals. *Brain Behav Immun* 27(1):101–108.
42. Cacioppo JT, et al. (2006) Loneliness within a nomological net: An evolutionary perspective. *J Res Pers* 40:1054–1085.
43. McCulloch CE, Searle SR, Neuhaus JM (2008) *Generalized, Linear, and Mixed Models* (Wiley, Hoboken, NJ).
44. Fredrickson BL, et al. (2013) A functional genomic perspective on human well-being. *Proc Natl Acad Sci USA* 110(33):13684–13689.
45. Fredrickson BL, et al. (2015) Psychological well-being and the human conserved transcriptional response to adversity. *PLoS One* 10(3):e0121839.
46. Tung J, et al. (2012) Social environment is associated with gene regulatory variation in the rhesus macaque immune system. *Proc Natl Acad Sci USA* 109(17):6490–6495.
47. Su AI, et al. (2004) A gene atlas of the mouse and human protein-encoding transcriptomes. *Proc Natl Acad Sci USA* 101(16):6062–6067.
48. Abbas AR, et al. (2005) Immune response in silico (IRIS): Immune-specific genes identified from a compendium of microarray expression data. *Genes Immun* 6(4):319–331.
49. Ingersoll MA, et al. (2010) Comparison of gene expression profiles between human and mouse monocyte subsets. *Blood* 115(3):e10–e19.
50. Cole SW, Yan W, Galic Z, Arevalo J, Zack JA (2005) Expression-based monitoring of transcription factor activity: The TELiS database. *Bioinformatics* 21(6):803–810.
51. Sloan EK, et al. (2007) Social stress enhances sympathetic innervation of primate lymph nodes: Mechanisms and implications for viral pathogenesis. *J Neurosci* 27(33): 8857–8865.
52. Leutenegger CM, et al. (2001) Real-time TaqMan PCR as a specific and more sensitive alternative to the branched-chain DNA assay for quantitation of simian immunodeficiency virus RNA. *AIDS Res Hum Retroviruses* 17(3):243–251.
53. Watson A, et al. (1997) Plasma viremia in macaques infected with simian immunodeficiency virus: Plasma viral load early in infection predicts survival. *J Virol* 71(1):284–290.
54. Lü X, et al. (1998) Targeted lymph-node immunization with whole inactivated simian immunodeficiency virus (SIV) or envelope and core subunit antigen vaccines does not reliably protect rhesus macaques from vaginal challenge with SIVmac251. *AIDS* 12(1): 1–10.
55. Fleiss JL (1981) *Statistical Methods for Rates and Proportions* (Wiley, New York).
56. Efron B, Tibshirani RJ (1993) *An Introduction to the Bootstrap* (Chapman & Hall, New York).